

Structure of the Homer EVH1 Domain-Peptide Complex Reveals a New Twist in Polyproline Recognition

Jutta Beneken,* Jian Cheng Tu,† Bo Xiao,†
Mutsuo Nuriya,† Joseph P. Yuan,†
Paul F. Worley,† and Daniel J. Leahy*‡§

*Department of Biophysics and Biophysical Chemistry

†Department of Neuroscience

‡Howard Hughes Medical Institute

Johns Hopkins University School of Medicine
Baltimore, Maryland 21205

Summary

Homer EVH1 (Ena/VASP Homology 1) domains interact with proline-rich motifs in the cytoplasmic regions of group 1 metabotropic glutamate receptors (mGluRs), inositol-1,4,5-trisphosphate receptors (IP3Rs), and Shank proteins. We have determined the crystal structure of the Homer EVH1 domain complexed with a peptide from mGluR (TPPSPF). In contrast to other EVH1 domains, the bound mGluR ligand assumes an unusual conformation in which the side chains of the Ser-Pro tandem are oriented away from the Homer surface, and the Phe forms a unique contact. This unusual binding mode rationalizes conserved features of both Homer and Homer ligands that are not shared by other EVH1 domains. Site-directed mutagenesis confirms the importance of specific Homer residues for ligand binding. These results establish a molecular basis for understanding the biological properties of Homer-ligand complexes.

Introduction

The Homer (ves1) family of proteins was initially identified in screens for proteins whose expression is upregulated in neurons following synaptic activity (Brakeman et al., 1997; Kato et al., 1997). Genes with this expression pattern, termed immediate-early genes (IEG), have generated interest as potential mediators of synaptic plasticity and thus learning and memory (Goebel et al., 1986). To date, one *Drosophila* and three mammalian Homer genes have been identified (Kato et al., 1998; Sun et al., 1998; Xiao et al., 1998). The mammalian Homer proteins localize to the postsynaptic density (PSD), where they appear to function as adaptor proteins that bind and cross-link cytoplasmic regions of group 1 metabotropic glutamate receptors (mGluRs), inositol-1,4,5-trisphosphate receptors (IP3Rs), and the recently discovered Shank proteins (Brakeman et al., 1997; Kato et al., 1998; Tu et al., 1998, 1999; Naisbitt et al., 1999).

The N-terminal ~110 amino acids of all Homer proteins show homology to EVH1/WH1 (Ena/VASP homology 1/Wiskott-Aldrich syndrome protein homology 1) domains found in the Ena/vasodilator-stimulated phosphoprotein (VASP) protein family (Gertler et al., 1996; Kato et al., 1997; Ponting and Phillips, 1997) as well as

the Wiskott-Aldrich Syndrome protein (WASP) and its neuronal homolog, N-WASP (Derry et al., 1994; Miki et al., 1996; Symons et al., 1996; Figures 1A and 1B). Homer EVH1 domains are highly conserved and bind a proline-rich "Homer ligand" motif present in mGluRs, IP3Rs, ryanodine receptors (RyRs), and Shank proteins (Tu et al., 1998, 1999; Naisbitt et al., 1999; Figure 1C). The original IEG form of Homer, termed Homer 1a, includes only 11 additional residues after the N-terminal EVH1 domain, while all other Homer proteins possess an extended C-terminal region of variable length predicted to adopt a coiled-coil (CC) structure. The CC region mediates homophilic and heterophilic interactions within the Homer family (Kato et al., 1998; Sun et al., 1998; Xiao et al., 1998; Tadokoro et al., 1999). All known functional properties of Homer proteins can be rationalized by the binding characteristics of the EVH1 and CC domains (Tu et al., 1998; Xiao et al., 1998).

EVH1 domains in other proteins also interact with polyproline-containing target sequences. The EVH1 domains of Ena and VASP recognize polyproline motifs in zyxin, vinculin, and the *Listeria monocytogenes* ActA protein (Niebuhr et al., 1997; Purich and Southwick, 1997). Interactions with zyxin and vinculin are essential for the proper function of Ena and VASP, which are found at sites of dynamic actin assembly and are thought to play an important role in the signal-induced reorganization of microfilaments (Reinhard et al., 1992, 1995; Brindle et al., 1996; Gertler et al., 1996; Ahern-Djamali et al., 1998; Lanier et al., 1999; Wills et al., 1999). Ena/VASP proteins have also been implicated in the actin-based motility of various intracellular bacterial pathogens, such as *Listeria* (Chakraborty et al., 1995; Gertler et al., 1996; Smith et al., 1996; Laurent et al., 1999).

The Homer ligand consensus sequence is PPxxF (Tu et al., 1998; Figure 1C). Single amino acid substitutions at the proline or phenylalanine positions disrupt Homer binding to short peptides or full-length mGluRs (Tu et al., 1998) or Shank proteins (Tu et al., 1999). This ligand specificity contrasts with that of Ena and VASP, which bind the sequence FPPPP (Niebuhr et al., 1997). Recently, crystal structures of the Mena (a murine Ena homolog) and EVL (Ena/VASP-Like) EVH1 domains complexed with proline-rich ligands have been determined (Fedorov et al., 1999; Prehoda et al., 1999). These structures reveal the FPPPP sequence bound in virtually identical fashion with the ligand forming a type II polyproline (PPII) helix (Figure 4A). Recognition of proline-rich ligands in PPII helical conformation is a feature of many protein-protein interactions, including those mediated by profilin, SH3, and WW domains (Musacchio et al., 1994; Yu et al., 1994; Macias et al., 1996; Mahoney et al., 1999). An interesting feature of the PPII helices is that they superimpose reasonably well when oriented either from N to C or C to N terminus, and both profilin and SH3 domains have been shown to bind ligands in both forward and reverse orientations (Feng et al., 1994; Mahoney et al., 1999). The presence of a conserved Phe in the Homer ligand on the opposite side of conserved prolines relative to the Ena/VASP ligands suggested that

§To whom correspondence should be addressed (e-mail: leahy@roucho.med.jhmi.edu).

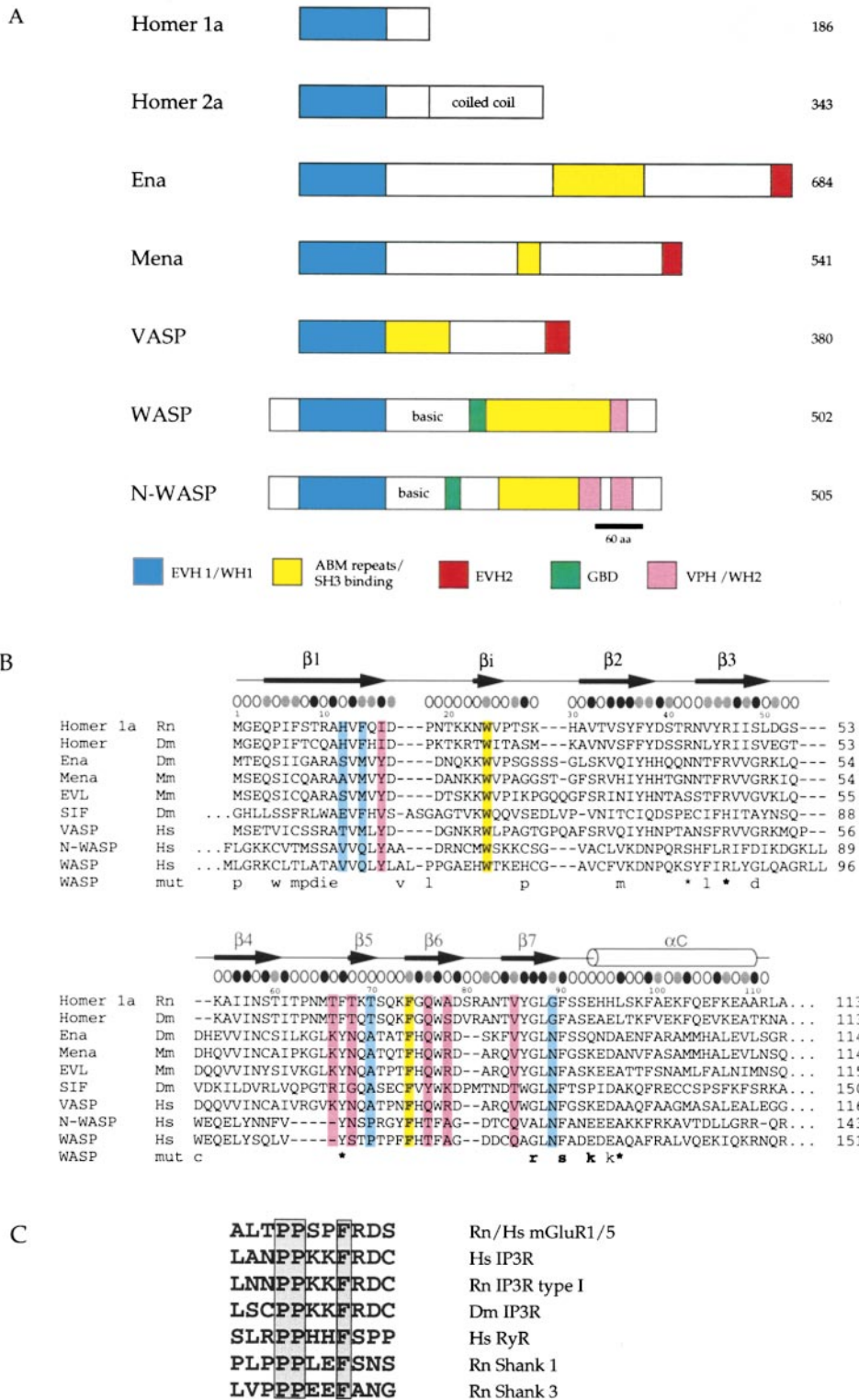


Figure 1. EVH1 Domains and Homer Ligand Sequences

(A) EVH1 domains are found at or near the N termini of Homer, Ena, Mena, VASP, and WASP proteins. Homer 1b/2/3 possess a C-terminal coiled-coil (CC) domain that mediates multimerization between various Homer proteins. The EVH1 domain in Ena, Mena, VASP, WASP, and N-WASP is followed by a central proline-rich region of variable length that contains docking sites for profilin (ABM-2 repeats) and SH3 domains (Purich and Southwick, 1997; Ramesh et al., 1999). The EVH2 regions mediate the multimerization of Ena, Mena, and VASP proteins (Ahern-Djamali et al., 1998). The G protein binding domain (GBD) of WASP and N-WASP interacts with the small G protein Cdc42 (Aspenstrom et al., 1996). The C-terminal verprolin homology domain (VPH) of N-WASP is necessary and sufficient for actin binding (Miki and Takenawa, 1998). The proteins are drawn to the scale shown, and the respective amino acid lengths are shown at the right.

Homer might bind ligand in an orientation opposite to that observed for Mena and EVL.

To elucidate the molecular nature of interactions between Homer and its ligands, we have determined the crystal structure of the rat Homer 1 EVH1 domain both alone and complexed with an mGluR-derived peptide. These structures reveal that the Homer EVH1 domain binds ligand in a unique manner that distinguishes it from other EVH1 domains and indeed from other PPII-binding proteins. The distinctive mode of Homer ligand binding minimizes the potential for cross-reaction with the many available proline-rich target sequences. Several residues of Homer are identified as key determinants of substrate specificity, and site-directed mutagenesis confirms their role in ligand recognition. Unexpectedly, several Homer mutants selectively bind mGluR versus Shank, indicating ligand-specific features of Homer-mediated interactions.

Results

Structure of the Homer EVH1 Domain

A fragment of rat Homer 1 encompassing residues 1–120 was expressed in *E. coli*, purified to homogeneity, and crystallized. The structure was determined to 1.7 Å limiting resolution utilizing multiwavelength anomalous diffraction (MAD) data collected from a single crystal of selenomethionyl-substituted (SeMet) protein. Only residues 1–111 were observed in this structure, and this shorter fragment of rat Homer 1 was expressed and cocrystallized with a synthetic peptide derived from mGluR (NH₂-TPSPF-CONH₂). Diffraction data to 1.9 Å limiting resolution were collected from a single orthorhombic crystal of the Homer-ligand complex, and the structure was solved by molecular replacement using the structure of the uncomplexed Homer EVH1 domain as a search model. The molecular replacement solution was used to calculate a F_o-F_c difference electron density map that revealed unambiguous density for all six residues of the bound peptide (Figure 3A). Data collection, phasing, and refinement statistics are shown in Table 1, along with stereochemical parameters of the final models.

A ribbon diagram of the Homer EVH1 domain with the bound peptide is shown in Figure 2A. No significant differences are observed between the structure of the EVH1 domain with and without bound peptide (104 α carbon atoms superimpose with an rmsd of 0.64 Å),

and all subsequent analyses reported here refer to the coordinates of the Homer-peptide complex. Superposition of the Homer, Mena, and EVL EVH1 domains reveals no significant topological differences. Eighty-five core α carbon atoms superimpose with an overall rmsd of 1.49 Å between Homer and Mena, 1.54 Å between Homer and EVL, and 0.71 Å between Mena and EVL.

EVH1 domains are structurally homologous to pleckstrin homology (PH) and phosphotyrosine-binding (PTB) domains, but PH and PTB domains bind ligands at sites unrelated to the EVH1 ligand binding site (Macias et al., 1994; Yoon et al., 1994; Zhou et al., 1995; Fedorov et al., 1999; Prehoda et al., 1999). Although PH domains exhibit very low levels of sequence conservation (<20% identity between family members), all PH domain structures are characterized by a highly polarized distribution of surface charge (Ferguson et al., 1994; Macias et al., 1994) that is believed to facilitate interactions with positively charged lipid membranes (reviewed in Lemmon and Ferguson, 1998). Unlike PH domains, the Homer EVH1 domain shows no concentrated regions of positive charge and does not bind ³H-IP3 in a centrifugation binding assay (data not shown).

Despite unequivocal structure similarity, no detectable sequence similarity exists between EVH1 domains and either PH or PTB domains, even when iterated search strategies such as PSI-BLAST (Altschul et al., 1997) are employed (Figure 1B). Overall, 12 out of 49 structurally homologous residues shared by EVH1, PH, and PTB domains occur at buried sites. This pattern of buried residues is especially conserved in β7 and αC (residues 86–103 in Homer 1) and allowed identification of a previously undetected EVH1 domain at the N terminus of the *Drosophila* protein Still Life (SIF) using a PHI-BLAST search (Zhang et al., 1998; Figure 1B). SIF is a 2064 amino acid protein found adjacent to the plasma membrane of synaptic terminals that interacts with Rho-like GTPases and participates in the organization of the actin cytoskeleton (Sone et al., 1997). Identification of an EVH1 domain in SIF suggests that this region may mediate interactions with a polyproline-containing ligand.

Comparison of Homer and Mena/EVL Peptide Binding

As shown in Figure 4A, the Mena and EVL EVH1 domains bind the core peptide FPPPP in an essentially identical PPII conformation within a homologous binding cleft.

(B) Sequence alignment of EVH1 domains. Species are indicated by Rn (rat), Hs (human), Mm (mouse), and Dm (*Drosophila*). Secondary structure elements of the Homer EVH1 domain are represented by arrows (β strands), cylinders (α helices), and lines (coils). Residues involved in ligand contacts are colored according to conservation among EVH1 domains: residues absolutely conserved between Homer and Mena/EVL sequences are highlighted in yellow, those conserved only among Homer sequences are colored blue, and those conserved only among Mena/EVL sequences only are colored pink. The Homer and Mena/EVL EVH1 domains have an overall sequence identity of ~30%, while the Mena and EVL EVH1 domains are 71% identical. The fractional solvent accessibility (FSA) of each residue in Homer 1a is indicated by ovals. Filled ovals = 0 ≤ FSA ≤ 0.1 (buried); shaded ovals = 0.1 < FSA ≤ 0.4 (partially accessible); open ovals = FSA > 0.4 (exposed). Missense mutations found in the EVH1 domain of the WASP gene are indicated in lower case letters below the WASP amino acid sequence. Mutations that are associated with the severe (classic) WAS phenotype are shown in bold letters (Zhu et al., 1997). Sites mutated to more than one residue are indicated by asterisks (S82P/F, R86C/H/P/L, Y107S/C, and A134T/V). Bold asterisks indicate residues that, when mutated, affect the interaction of WASP with WIP (Stewart et al., 1999). Gaps are indicated by dashes while continued sequences at N- and C-termini are indicated by periods. Residue numbering for Homer 1a is shown above its amino acid sequence. The number of the last included residue of each protein is shown at the end of each row.

(C) Alignment of Homer EVH1 ligand sequences from mGluR, IP3R, RyR, and Shank proteins, highlighting the residues absolutely required for recognition that define the consensus Homer ligand motif PPxxF (Tu et al., 1998, 1999).

Table 1. Data Collection, Phase Calculation, and Refinement Statistics

	SeMet Homer EVH1 (MAD Data)				EVH1 + Peptide
Resolution limits (Å)	30.0–1.7				30.0–1.9
Wavelength (Å)	0.9879	0.9793	0.9790	0.9611	1.5418
Unique reflections	24051	24179	24226	24479	7996
Redundancy	4.8	4.8	4.8	4.9	7.3
Completeness (%)	96.8	97.2	97.3	98.4	98.3
($\langle I \rangle / \langle \sigma I \rangle$) ^a	21.5 (2.3)	21.0 (2.1)	20.9 (2.0)	20.4 (1.9)	28.0 (5.1)
R _{sym} (%) ^a	8.1	8.7	9.1	8.8	8.8
Overall figure of merit	0.71				
Correlation coefficient ^b					41.7
R (%) ^b					46.5
MAD Structure Factor Ratios ^c and Anomalous Scattering Factors ^d					
Wavelength (Å)	0.9879	0.9793	0.9790	0.9611	
0.9879	0.033	0.040	0.032	0.026	
0.9793		0.047	0.029	0.044	
0.9790			0.063	0.036	
0.9611				0.050	
f' (e)	−4.87	−9.96	−8.06	−4.15	
f'' (e)	0.47	3.77	6.28	4.12	
Refinement Statistics ^e					
Resolution limits (Å)	30.0–1.7		30.0–1.9		
R _{cryst} (%)	24.5		24.1		
R _{free} (%)	28.5		28.9		
Average B (Å ²) protein	19.0		24.7		
solvent	39.1		44.3		
peptide	—		25.9		
No. of water molecules	88		76		
Rmsd bond lengths (Å)	0.0126		0.0187		
Rmsd bond angles (°)	1.745		1.924		
Rmsd B values (Å ²)					
bonds/angles main chain	1.739/2.560		1.611/2.296		
bonds/angles side chains	2.553/3.659		2.402/3.308		

^a Values in parentheses are for the highest resolution shell. $R_{sym} = 100 \times \sum |I - \langle I \rangle| / \sum I$, where I is the integrated intensity of a given reflection summed over the entire unit cell.

^b R value = $\sum |F_o(obs) - F_p(calc)| / \sum F_o(obs)$, where F_p is the structure factor amplitude.

^c RMS ($\Delta|F|$)/RMS ($|F|$), where $\Delta|F|$ is the Bijvoet difference at one wavelength (values on the diagonal) or the dispersive differences between two wavelengths (values off the diagonal).

^d Anomalous components of the Se scattering factors as a function of wavelength as determined by SOLVE (Terwilliger and Eisenberg, 1983).

^e Final rounds of refinement included all data. The free R value was calculated from 10% of the data excluded from the refinement (Brunger, 1992a).

Superposition of the α carbon positions of eight ligand-contacting residues of Mena and EVL results in the superposition of the bound ligand atoms with an rmsd of 0.72 Å for all equivalent atoms, and superposition of the bound ligands alone results in an rmsd of 0.51 Å for all

equivalent atoms. In contrast, the ligand bound to Homer (TPPSPF) occupies a partially overlapping but distinct binding site (Figure 4B). While the Homer and Mena/EVL ligands are bound in the same orientation, they overlap only in a pair of tandem prolines (Pro-2/Pro-3

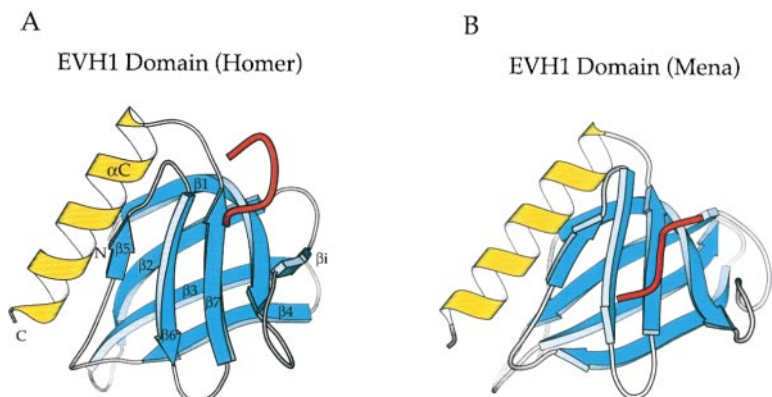
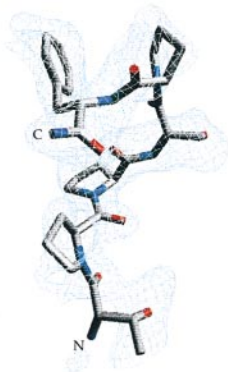


Figure 2. Structural Comparison of Homer and Mena EVH1 Domains

Ribbon diagrams of the (A) Homer and (B) Mena EVH1 domains (Prehoda et al., 1999) with bound ligands shown in red. Both molecules are shown in a similar orientation. This figure, as well as Figure 3B, was prepared using MOLSCRIPT (Kraulis, 1991).

A



B

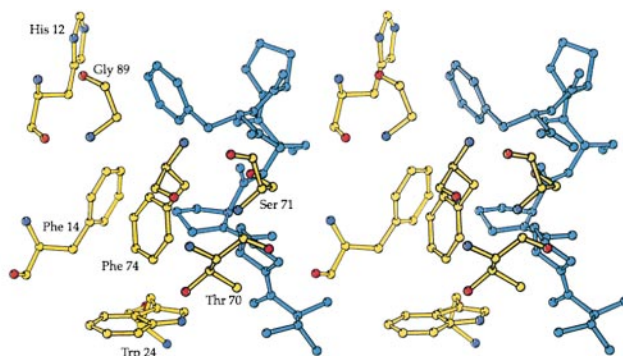


Figure 3. Structure and Environment of the Homer Ligand

(A) F_o-F_c difference electron density map calculated at 1.9 Å resolution using coefficients calculated from the initial molecular replacement solution, contoured at 1.7σ and superimposed with the final model for the bound ligand TPPSPF. This figure was prepared using SETOR.

(B) Stereo diagram of the Homer ligand binding site showing protein residues (yellow) with side chains within 3.85 Å of the bound ligand (blue). The conserved proline residues of the ligand (Pro-2 and Pro-3) adopt a PPII conformation. Ser-4, Pro-5, and Phe-6 form a type VIa beta turn, positioning the conserved phenylalanine on the same face of the ligand as the conserved proline residues. This face of the ligand interacts with the protein while the side chains of the nonconserved Ser-4 and Pro-5 are exposed to solvent. When calculated in the absence and presence of the Homer protein, the fractional solvent accessibilities of Pro-2, Pro-3, and Phe-6 decrease from 0.61, 0.85, and 0.70 to 0.17, 0.13, and 0.16, respectively, while the fractional solvent accessibilities of Ser-4 and Pro-5 remain unchanged at 1.0 and 0.83, respectively.

of the Homer ligand and Pro-4/Pro-5 of the Mena/EVL ligand). Unique features of EVH1 domain–ligand interactions that differentiate the Homer and Mena/EVL subfamilies are found on opposite sides of these prolines.

The N-terminal threonine of the bound Homer peptide does not directly contact the protein, and the amino acid at this position is highly variable among Homer ligand sequences (Figure 1C). Thr-1, Pro-2, Pro-3, and Ser-4 of the bound Homer peptide adopt the PPII conformation, but Ser-4 also occupies the second position of a type VIa beta turn comprising residues Pro-3, Ser-4, Pro-5, and Phe-6 (Figure 3). Type VIa beta turns require a *cis*-proline at the third position, and this feature is observed in the bound Homer ligand. The tight turn positions the side chains of Ser-4 and Pro-5 away from the protein surface and exposes them to solvent. These residues occupy positions in the ligand that are highly divergent between different Homer targets (Figure 1C). For example, the amino acids at these positions are Lys–Lys in IP3Rs and Leu–Glu or Glu–Glu in Shanks. Failure to conserve a proline at position 5 in Homer target sequences indicates that a type VIa tight turn is not a specific structural requirement for bound Homer ligands. It is likely, however, that a tight turn is required for appropriate positioning of the conserved phenylalanine and proline residues.

The conserved Phe-6 at the C terminus of the bound Homer ligand is substantially buried between the Homer protein and the residues of the peptide tight turn (Figures 3B and 4B). The side chain of Phe-6 directly abuts the α carbon position of Gly-89 in the Homer protein (Figure 3B), and any models that substitute residues other than glycine at this position generate substantial steric clashes. Glycine is conserved at this position in all

Homer sequences, but bulkier amino acids are found at this position in all non-Homer EVH1 domains (Figure 1B).

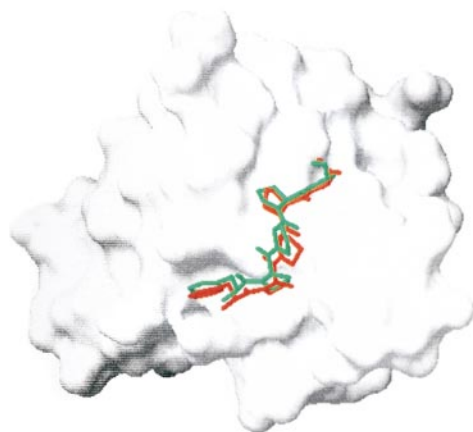
Mutagenesis of Homer Binding Site Residues

To determine the importance of specific residues for ligand binding, several Homer EVH1 point mutants were constructed and assayed for ligand binding (Figure 5). To test whether a glycine at position 89 is required to accommodate the ligand phenylalanine, Gly-89 was mutated to either alanine or asparagine. Ena/VASP, as well as most other EVH1 domain proteins, naturally possess asparagine at this position. Substitution of either alanine or asparagine eliminated detectable binding of Homer EVH1 to both mGluR1 and Shank 3, thus identifying Gly-89 as a key determinant of Homer ligand specificity.

To examine the relevance of proline interactions, three of the four critical proline contact sites in Homer were mutated (Trp-24, Thr-70, and Phe-74, but not Phe-14). Mutation of Phe-74 and Trp-24 to alanine disrupted binding to both Shank 3 and mGluR1. In contrast, mutation of Trp-24 to tyrosine selectively disrupted binding to mGluR1 but not to Shank 3. Mutation of Thr-70 to glutamic acid disrupted binding to Shank 3 but not to mGluR1, while mutation of Thr-70 to alanine did not affect binding to either ligand. The target selectivity of the W24Y and T70E mutations suggests a role for ligand-specific features in Homer-mediated interactions. The failure of the T70A mutation to disrupt ligand binding may reflect that, in contrast to the T70E mutation, replacement of a larger amino acid with a smaller amino acid is potentially less deleterious than vice versa and results in an effect on ligand binding that is too small to be detected by our assay.

In the Mena and EVL EVH1 domain structures, the

A



B

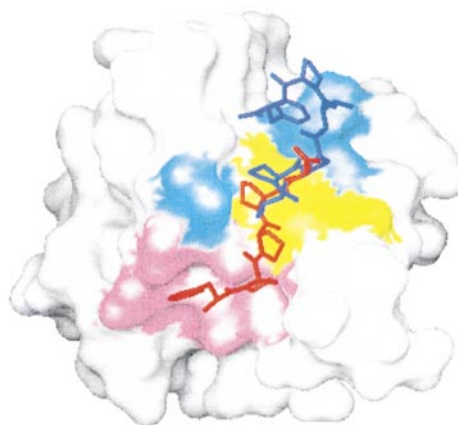


Figure 4. Structural Comparison of Homer and Mena/EVL Peptide Binding

(A) Surface representation of the Mena EVH1 domain with bound Mena (red) and EVL (green) ligands shown as a stick representation. Only the core FPPPP residues of the bound EVL ligand are shown for ease of comparison with the bound Mena ligand. The orientation of the EVH1 domain in both panels is identical to that in Figures 2 and 5B.

(B) Surface representation of the Homer EVH1 domain with the bound Homer peptide shown in blue. The Mena ligand is shown in red in its relative position on the Homer surface. Residues involved in ligand contacts are colored according to conservation among EVH1 domains: residues absolutely conserved between Homer and Mena/EVL sequences are highlighted in yellow (Trp-24 and Phe-74), those conserved only among Homer sequences are colored blue (His-12, Phe-14, Thr-70, and Gly-89), and those conserved only among Mena/EVL sequences are colored pink (Ile-16, Thr-66, Thr-68, Gln-76, Ala-78, and Val-85). Residues highlighted in this figure are also indicated with the same color scheme in Figure 1B. This figure, as well as Figures 5B and 6, was prepared using GRASP (Nicholls et al., 1991).

conserved ligand phenylalanine makes contacts with Lys-69, Gln-79, Asn-71, Arg-81, and Val-86 (Mena numbering). The equivalent residues in Homer do not make ligand contacts, and only two are preserved: Gln-76 (equivalent to Gln-79 in Mena) and Val-85 (Val 86 in Mena). Mutation of Gln-76 to alanine or arginine did not alter Homer ligand binding, while mutation of Val-85 to alanine diminished Homer binding to mGluR1, but not to Shank 3. The effects of the V85A mutation on Homer binding to mGluR1 may be indirect, as Val-85 directly contacts Trp-24, a key ligand contact residue.

The surface locations of the residues mutated in the Homer EVH1 domain are shown in Figure 5B. With the exception of V85A, all mutations that affect Homer ligand binding make direct van der Waals contacts with the bound peptide (see also Figure 3B). Prior to solving the structure of the Homer EVH1-ligand complex, we tested a series of Homer point mutations based on reported mutations of the WASP EVH1 domain that produce severe phenotypes (Figures 1B and 6). A number of solvent-exposed hydrophobic residues were also selected as mutagenesis targets. Mutations that did not affect binding include: F7R, S8L, N23A, S28A, S35V, D39E, R42A, R42E, R46A, I48A, N64G, F69A, Q72A, E93K, H95A, and L96S (data not shown).

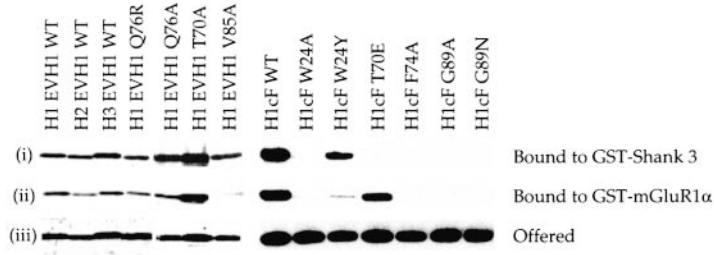
Discussion

We have determined the high-resolution crystal structures of the rat Homer 1 EVH1 domain both alone and

complexed with the mGluR-derived peptide TPPSPF. These structures reveal peptide bound to the Homer domain in a different manner than has been observed for the Mena and EVL EVH1 domains (Fedorov et al., 1999; Prehoda et al., 1999). Distinctive regions of the Homer and Mena/EVL domains make ligand contacts, and the Homer ligand, unlike the Mena/EVL ligands, does not adopt the PPII conformation throughout its length. Instead, the Homer ligand possesses a tight beta turn between key protein-contacting residues. The Homer and Mena/EVL EVH1 domains do, however, share a homologous region that interacts with tandem prolines. These results, combined with mutagenesis studies, explain different target specificities among EVH1 domains and identify residues important for discriminating modes of substrate binding.

Conservation of sequence, structure, and polyproline recognition between the Homer and Mena/EVL EVH1 domains strongly suggests that these domains are derived from an ancestral polyproline-binding protein. Polyproline sequences possess unique structural features that appear to favor their selection as binding targets. The covalent bond between the proline side chain and main chain greatly reduces the main chain torsional conformations available to proline and strongly favors the PPII helical conformation, which is observed for polyproline in solution (Kurtz et al., 1956; Stapley and Creamer, 1999). Binding of a preformed structure to a protein results in a substantially smaller loss of configurational entropy upon binding than would occur for a random

A



B

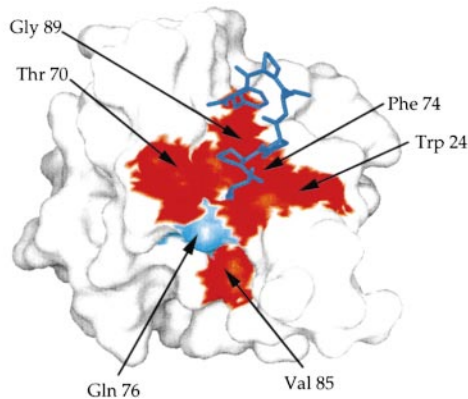


Figure 5. Homer Site-Directed Mutagenesis

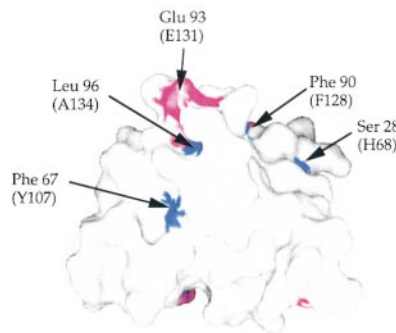
(A) Immunoblot probed with pan-Homer 1 antibody showing mutants of Homer 1 EVH1 domains (H1 EVH1) and full-length Homer 1c (H1c) offered (iii) and bound to immobilized GST-Shank 3 (i) or GST-mGluR1 α (ii). All mutants expressed at normal levels. Q76R, Q76A, and T70A exhibit normal binding, while V85A, W24A, W24Y, T70E, F74A, G89A, and G89N disrupt detectable binding to either or both ligands. Positive control experiments with wild-type proteins are indicated.

(B) Surface representation of the Homer EVH1 domain showing the location of residues targeted by site directed mutagenesis. Mutations that disrupt binding of Homer EVH1 to either of two ligands (GST-mGluR1 α or GST-Shank 3) are shown in red, while those that have no effect on binding are shown in light blue. The Homer ligand is shown in dark blue.

peptide and thus requires fewer specific interactions to compensate for the entropic cost of binding (Petrella et al., 1996). The utility of this property of proline-rich

sequences is reflected in the fact that profilin, EVH1, SH3, and WW domains have all been shown to bind peptides in the PPII conformation, despite otherwise

A



B

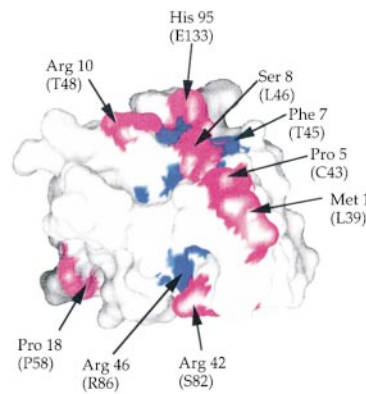


Figure 6. Mapping of WASP-Causing Mutations on the EVH1 Surface

(A and B) Surface representations of the Homer 1 EVH1 domain with sites homologous to positions of WASP mutations (in parentheses) colored according to solvent accessibility. Solvent exposed residues are shown in magenta, and buried or partially buried residues are shown in blue. Mutations of residues R86, Y107, and A134 have been shown to disrupt the interaction of WASP with WIP (Stewart et al., 1999). The sites and nature of WASP mutations (Schwartz et al., 1996), the alignment of these mutations with the Homer sequence, and their solvent exposure within the Homer EVH1 domain are indicated in Figure 1B. The orientation of the EVH1 domain in (A) is identical to that in Figure 2A. In (B), the molecule is rotated $\sim 180^\circ$ about the vertical axis.

unrelated structures (Musacchio et al., 1994; Yu et al., 1994; Macias et al., 1996; Fedorov et al., 1999; Mahoney et al., 1999; Prehoda et al., 1999). The 2-fold pseudosymmetry of PPII helices also has implications for interactions with proteins in that a binding site selected to recognize PPII helices may in some instances bind target peptides in either orientation. Profilin and SH3 domains, for example, have been shown to bind different proline-rich sequences in opposite orientations, with the polarity of the bound peptide determined by nonproline residues (Feng et al., 1994; Mahoney et al., 1999; reviewed in Kuriyan and Cowburn, 1997).

Given these features of proline-rich sequences, two aspects of the interaction between Homer and the mGluR1 peptide are notable. First, unlike all other examples of recognition of proline-rich targets, the mGluR1 peptide does not adopt the PPII conformation throughout its length but rather incorporates a tight beta turn at its C terminus. This tight turn appears necessary for the appropriate positioning of the conserved prolines and phenylalanine of the ligand with the Homer domain (Figures 3B and 4B) and is thus likely to be a feature of all Homer–ligand interactions. Second, by analogy with profilin and SH3 domains, the placement of a conserved phenylalanine before prolines in Mena/EVL targets and after prolines in Homer targets suggested that Homer EVH1 domains might bind ligands at a site homologous to the Mena/EVL binding site but with the main chain oriented in the opposite direction. However, the Homer EVH1 domain interacts with the mGluR1 peptide in the same orientation as that observed for the Mena/EVL EVH1 domains. While both domains use a shared region for interactions with prolines, unique sites within these domains are utilized for crucial interactions with nonproline residues.

The use of distinct but overlapping binding sites poses unique challenges to the generation and maintenance of substrate specificity. Not only must key ligand contact residues be conserved, but residues in regions that contact ligand in Homer but not in Mena/EVL must be selected against in Mena/EVL to avoid cross-reaction with Homer ligands and vice versa. Comparison of the Homer and Mena/EVL peptide binding sites reveals residues that are conserved among all EVH1 domains as well as residues that are conserved only among subsets of EVH1 domains and are strictly absent from other EVH1 domains (Figures 1B and 4B). Residues that contact the ligand in the overlapping region of the Homer and Mena/EVL ligand binding sites are conserved in all EVH1 domains and include Trp-24 and Phe-74 (following a Homer numbering convention). Conversely, residues contacting the unique N-terminal regions of the Mena/EVL ligands (Tyr-16, Lys-69, Asn-71, Gln-79, Arg-81, and Val-86 [Mena numbering]) are conserved in Mena and EVL, while identical homologs of only Gln-79 and Val-86 are present in Homer proteins. Residues in Homer that contact the unique C-terminal phenylalanine of the Homer ligand (including His-12, Phe-14, Thr-70, and Gly-89 [Homer numbering]) are exclusively present in Homer EVH1 domains.

Analysis of binding properties of Homer EVH1 point mutants generally confirms the importance of these critical contact sites. In particular, the phenylalanine in the Homer ligand packs directly on Gly-89 in a manner that

suggests any other residue at this site would interfere with this interaction (Figure 3B), and mutation of this residue to either alanine or asparagine eliminates detectable binding of Homer to its substrates (Figure 5A). The absence of an unusual ϕ angle at Gly-89 suggests that nonglycine residues at this position would not require major changes in backbone conformations. All non-Homer EVH1 domains possess an amino acid other than glycine at this position (typically asparagine, see Figure 1B), indicating that these domains are unlikely to bind peptide in the same manner as Homer and that a nonglycine residue at this position may be conserved in part to avoid cross-reaction with Homer substrates. Conversely, amino acid differences in Homer residues not involved in ligand contacts but equivalent to positions of Mena/EVL ligand contact residues (Ile-16/Tyr-16, Thr-66/Lys-69, Thr-68/Asn-71, and Ala-78/Arg-81 [Homer/Mena numbering]) may have been selected to prevent cross-reaction with Mena/EVL substrates.

Another residue with potential to discriminate between Homer and Mena/EVL binding modes is Thr-70 (Homer numbering). As shown in Figure 4B, the ligand prolines that bind to homologous sites in the Homer and Mena/EVL proteins (Pro-2 and Pro-3 in the Homer ligand and Pro-4 and Pro-5 in the Mena/EVL ligands) are shifted by ~ 2 Å relative to one another following superposition of the Homer and Mena EVH1 domains. This shift appears to be due in part to Thr-70 in the Homer protein, which contacts Pro-2 of the Homer ligand but would clash with a peptide bound in the Mena/EVL-like position. Thr-70 is conserved in all Homer proteins, while the residue at the homologous position in the Mena/EVL subfamily of EVH1 domains is alanine, which accommodates the relative shift of the bound peptides. Mutation of Thr-70 to alanine in Homer does not disrupt ligand binding (see Figure 5A) but may be conserved in Homer EVH1 domains in part to prevent interactions with Mena/EVL substrates.

Our studies identified Homer mutants that selectively bind mGluRs or Shank. When Trp-24 is mutated to tyrosine, the resulting Homer mutant binds Shank 3, but not mGluRs. Similarly, Homer V85A binds Shank 3 but not mGluRs. By contrast, T70E binds mGluRs but not Shank 3. The selectivity of these mutants may result from slight differences in either the topology or energetics of the contacts between Homer and the prolines of these ligands. These examples indicate that in addition to the core consensus residues there are determinants of Homer binding that are ligand specific.

Residues conserved only in subsets of Homer ligands may also be instructive. The amino acids at positions xx of the PPxxF Homer ligand motif exhibit extreme variability between different families of receptors (Figure 1C). In screens of random peptide libraries, amino acids at these positions are not conserved (P. W. et al., unpublished data), suggesting that they are not important for binding to EVH1 domains. On the other hand, residues at these positions are absolutely conserved among divergent members of each receptor family. For example, Lys-Lys is found at these positions in the IP3R sequences of nematodes, flies, frogs, rats, and humans, suggesting that these residues may be important for some additional function. One possibility is that when

bound to Homer, these residues constitute a new binding surface that mediates receptor type-specific interactions with additional molecules.

The EVH1 domain structures of Homer and Mena/EVL may be used to evaluate the homologous EVH1 domain in WASP, for which no structural information is currently available. The WASP EVH1 domain is the target of mutations in Wiskott-Aldrich syndrome (WAS) (Derry et al., 1994) and, like Ena and VASP, appears to link extracellular signals to cytoskeletal assembly (Aspenström et al., 1996; Kolluri et al., 1996; Miki et al., 1996; Symons et al., 1996; Miki and Takenawa, 1998). WASP expression is restricted to hematopoietic cells, and WAS, which is characterized by eczema, thrombocytopenia, immunodeficiency, and an increased risk of lymphoid malignancies, results from defects in these cells (Nonoyama and Ochs, 1998; Ramesh et al., 1999; reviewed in Kirchhausen, 1998). The molecular function of WASP involves direct interactions with multiple proteins, including Cdc42 (Aspenström et al., 1996; Symons et al., 1996), WIP (Ramesh et al., 1997), Nck (Rivero-Lezcano et al., 1995), Grb2 (She et al., 1997; Zhu et al., 1997), phospholipase C- γ (Cory et al., 1996; Zhu et al., 1997), and several kinases (Banin et al., 1996; Bunnell et al., 1996; Cory et al., 1996; Zhu et al., 1997). These interactions appear to play a role in cytoskeletal assembly, since the T cells and platelets of WAS patients exhibit cytoskeletal abnormalities, and disruption of these interactions is likely to be a feature of many, if not all, WAS-causing mutations.

Surface representations of the Homer EVH1 structure with the location of sites homologous to disease-causing mutations in the WASP EVH1 domain highlighted in color are shown in Figure 6. Most WASP mutations map on or near one face of the EVH1 domain, and those that do not map to this face invariably occur at sites of buried residues. Mutations that impair binding properties of proteins generally fall into two categories: those that disrupt global structure and those whose effects are localized to a specific active site or binding interface. Mutations that result in global disruptions typically occur at buried hydrophobic positions or affect residues that perform key structural roles. Such mutations often exhibit no essential relation to a protein-active site. Mutations with local effects frequently map to surface-exposed sites that cluster within a specific region of the protein surface. The majority of surface-exposed WASP mutations are found in a location that is opposite to the ligand binding site in the Homer and Mena/EVL EVH1 domains (Figure 6). Moreover, several WASP mutations were tested in Homer and did not disrupt binding to Homer ligands. This strongly suggests that the WASP EVH1 domain interacts with ligands at different sites than the Homer and Mena/EVL EVH1 domains.

The structure of the Homer EVH1 domain with bound peptide adds a new twist to the binding modes of EVH1/PH/PTB domains and rationalizes conserved residues in both EVH1 domain subsets and their targets. Among EVH1 domains, Homer proteins appear to be unique in their mode of ligand recognition and represent a distinct functional subset of these domains. While the principal elements of ligand binding and recognition by the Homer and Mena/EVL subfamilies of EVH1 domains seem well understood, future work will be needed to elucidate the

contributions from both protein and ligand that give rise to more subtle ligand preferences within members of both subfamilies.

Experimental Procedures

Protein Expression and Purification

Residues 1–120 or 1–111 of rat Homer 1a were expressed in *Escherichia coli* BL21 cells as a C-terminal fusion to glutathione-S-transferase (GST-1aEVH) as previously described (Tu et al., 1998). Selenomethionine-substituted (SeMet) GST-1aEVH was prepared by expression in the methionine auxotrophic strain B834 (DE3) (Novagen). Five milliliters of an overnight culture grown at 37°C in LB media supplemented with 100 μ g/ml ampicillin (Sigma) were added to 4 liters M9 minimal media (GIBCO-BRL) supplemented with the following: 100 μ g/ml ampicillin, 0.05 mg/ml alanine, aspartic acid, glutamic acid, phenylalanine, glycine, histidine, isoleucine, lysine, asparagine, proline, glutamine, arginine, serine, threonine, valine, tryptophan, tyrosine, L-selenomethionine, 1 μ g/ml thiamine (Sigma), 2 mM MgSO₄, 1% glucose, and 100 mM CaCl₂. Cells were grown to an OD₆₀₀ of 0.5 at which time IPTG (Calbiochem) was added to a final concentration of 0.2 mM. Cells were grown for an additional 3 hr, harvested by centrifugation, and resuspended in PBS/1% Triton. Pepstatin A and leupeptin (Boehringer-Mannheim) were added to a final concentration of 1 μ g/ml, and PMSF (Life Technologies) was added to 0.5 mM. Cells were lysed by sonication and centrifuged at 13,000 rpm in an SS-34 rotor to pellet cell debris. The cleared lysate was added to a 5 ml glutathione-agarose (Sigma) column. The column was washed in succession with 20 column volumes of PBS/1% Triton, 20 column volumes of PBS, and 10 column volumes of cleavage buffer (50 mM Tris [pH 7.4], 150 mM NaCl, 2.5 mM CaCl₂, 50 mM 2-mercaptoethanol). All buffers were degassed. A 50% slurry of glutathione-agarose beads loaded with fusion protein was incubated with 20 units of biotinylated Thrombin (Novagen) for 16 hr at room temperature. The released cleavage product (1a-EVH) was collected, and the biotinylated Thrombin was removed with streptavidin-agarose beads (Novagen). 1a-EVH was further purified by cation-exchange chromatography using a ResourceS column (Amersham-Pharmacia). Peptides corresponding to hexamer and decamer consensus sequences from mGluR, Shank, and IP3 were synthesized on a PE Biosystems 430A peptide synthesizer using Fmoc chemistry, purified by reverse-phase HPLC, and analyzed by mass spectrometry.

Crystallization and Data Collection

Crystals of native and SeMet protein alone and native protein-peptide complex were grown in hanging drops by the vapor diffusion method (Wlodawer et al., 1975). Crystals of the unliganded protein were grown by mixing 1 μ l of a 9 mg/ml solution of native or SeMet 1aEVH 1–120 with a 1:1 dilution of reservoir buffer (30% PEG 3350, 87 mM MgSO₄, 50 mM HEPES [pH 7.3]) with distilled water and equilibrating over 1 ml of reservoir buffer. All crystallization trials for the SeMet protein were set up under anaerobic conditions to minimize potential problems due to oxidation. Crystals of the protein-peptide complex were grown by mixing 1 μ l of a ~20 mg/ml solution of native 1aEVH 1–111 and 1 μ l of 10 mg/ml peptide with a 1:1 dilution of reservoir buffer (30% PEG 3350, 100 mM Sodium Acetate, 100 mM Tris [pH 8.0]) with distilled water. We observed two different crystal forms for both the native and the SeMet unliganded protein. Crystals in the orthorhombic space group P2₁2₁2₁ (unit cell dimensions: a = 33.79 Å, b = 51.40 Å, c = 66.30 Å) typically grew to a size of 0.5 mm \times 0.03 mm \times 0.03 mm. Crystals in the trigonal space group P3₂21 (unit cell dimensions: a = b = 49.94 Å, c = 80.91 Å) grew to a size of 0.4 mm \times 0.1 mm \times 0.1 mm. Crystals of the protein-peptide complex grew in space group P2₁2₁2₁ to a maximum size of 0.55 mm \times 0.28 mm \times 0.01 mm. All data used for phasing and refinement of the unliganded protein were collected from a single trigonal SeMet crystal soaked in mother liquor plus 10% (v/v) ethylene glycol for approximately 3 min prior to flash freezing in a gaseous nitrogen stream at –180°C. X-ray diffraction data suitable for multiwavelength anomalous dispersion (MAD) phasing were collected at four wavelengths at or near the Se absorption edge. These data were collected at beamline X4A of the National

Synchrotron Light Source at Brookhaven National Laboratory using an R-AXIS IV image plate detector. Nonoverlapping oscillations (2°) at ϕ and $\phi + 180^\circ$ were measured over a 90° rotation of the crystal, interleaving the four wavelengths. Data used to solve the protein-peptide complex were collected from a single crystal flash frozen at -180°C , using $\text{CuK}\alpha$ radiation generated by a Rigaku RU-200 generator and an R-AXIS IV image plate detector. Nonoverlapping oscillations (1.5°) were measured over a 247° rotation of the crystal. All data were processed and scaled using the DENZO/SCALEPACK programs (Otwinowski and Minor, 1997). Data collection statistics for the unliganded protein and the protein-peptide complex are shown in Table 1.

Structure Solution and Refinement

The two expected selenium sites in the unliganded protein were determined and refined using the program SOLVE (Terwilliger and Eisenberg, 1983; Terwilliger and Berendzen, 1997) and initial Se scattering factors from Hall et al. (1997). Values for the Se scattering factors as refined by SOLVE are shown in Table 1. The experimental MAD phases were improved by solvent flattening and histogram matching using DM (Collaborative Computational Project, 1994). An initial model of residues 1–105 was built into 1.8 Å experimental electron density maps using the program O (Jones et al., 1991). The model was refined with maximum-likelihood targets in CNS (Pannu and Read, 1996; Brünger et al., 1998) using data to 1.7 Å limiting resolution collected at 0.9879 Å. Eight rounds of model building and water addition alternated with B-factor and positional refinement yielded the current model, which includes residues 1–111 and 88 water molecules. No electron density was observed for residues 112–120. The final model has a crystallographic R value of 24.5% and a free R value of 28.5%. The solvent content is 41%, with one molecule per asymmetric unit. Fractional solvent accessibility for each residue was calculated in X-PLOR (Brünger, 1992b). The structure of the Homer EVH1-peptide complex was solved by molecular replacement using AMoRe (Navaza, 1994) using the refined model of the unliganded protein as the search model. The top molecular replacement solution has a correlation coefficient of 41.7 and an R value of 46.5%. This model was successively subjected to rigid body, simulated annealing, and positional refinement using data to 1.9 Å limiting resolution. Prior to addition of any ligand components to this refined molecular replacement model, a difference electron density map with sigma α -weighted $F_o - F_c$ coefficients (Read, 1986) was calculated and revealed unambiguous density for all ligand residues. Several rounds of model rebuilding and water addition, alternated with positional and individual B-factor refinement, yielded the current model of residues 6–109 of the Homer EVH1 domain, all six peptide residues, and 76 water molecules. No electron density was observed for Homer residues 1–5 or 110–111. Throughout this refinement, no evidence of minor alternative conformations for the bound peptide was observed. The final model has a crystallographic R value of 24.1% and a free R value of 28.9%. The solvent content is 31%, with one molecule per asymmetric unit. Both the unliganded protein and protein-ligand models were analyzed by the program PROCHECK (Laskowski et al., 1993), and all stereochemical parameters show equal or less variance from ideal values when compared with other structures determined at similar resolution. No main chain torsion angles are found in energetically unfavorable positions, although a *cis*-peptide bond is found between Ser-4 and Pro-5 of the ligand. Refinement statistics for the unliganded protein and the protein-ligand complex are shown in Table 1. The agreement statistics seem slightly high for structures at this resolution, but $F_o - F_c$ difference electron density maps exhibit no significant unexplained features, and the high quality of the experimental maps provide confidence in the accuracy of these structures. Efforts are currently underway to adjust refinement parameters to further reduce the free R value.

Site-Directed Mutagenesis and In Vitro Binding

Point mutants of N-terminal myc-tagged Homer 1 EVH1 domains and full-length Homer 1c were made using the QuikChange TM Site-Directed Mutagenesis Kit (Stratagene). Expression constructs were transiently transfected into HEK293 cells using calcium phosphate methods. Cell lysates were prepared 24–48 hr posttransfection in

PBS/1% Triton X-100 (Sigma) and protease inhibitors. GST pull-down assays were performed by mixing 100 μl of cell lysate with GST-mGluR1 α (mGluR1 α residues 1104–1199) and GST-Shank 3 (Shank 3 residues 1269–1408; Tu et al., 1999) bound to glutathione-agarose, incubating at 4°C for 2 hr, and washing with PBS and PBS/1% Triton X-100. Bound products were eluted with 100 μl 2 \times SDS loading buffer and detected by SDS-PAGE and immunoblot using pan-Homer 1 antibody and ECL reagents (Amersham).

Acknowledgments

We thank C. Dann, K. Ramyar, C. Ogata, and the staff at beamline X4A for their assistance in data collection; the JHMI DNA/Protein/Peptide Facility for peptide synthesis and purification; S. Gabelli for her assistance with AMoRe; W. Lim for suggesting the use of minimal peptides for cocrystallization. This work was supported by grants to P. F. W. from the National Institute on Drug Abuse and the National Institute of Mental Health and to D. J. L. from the National Institutes of Health. D. J. L. is an assistant investigator of the Howard Hughes Medical Institute. We also wish to acknowledge a special debt to the late Daniel Nathans for inspiring and supporting early stages of this work; he is sorely missed.

Received May 10, 1999; revised January 21, 2000.

References

- Ahern-Djamali, S.M., Comer, A.R., Bachmann, C., Kastenmeier, A.S., Reddy, S.K., Beckerle, M.C., Walter, U., and Hoffmann, F.M. (1998). Mutations in *Drosophila* enabled and rescue by human vasodilator-stimulated phosphoprotein (VASP) indicate functional roles for Ena/VASP homology domain 1 (EVH1) and EVH2 domains. *Mol. Biol. Cell* 9, 2157–2171.
- Altschul, S.F., Madden, T.L., Schaffer, A.A., Zhang, J., Zhang, Z., Miller, W., and Lipman, D.J. (1997). Gapped BLAST and PSI-BLAST: a new generation of protein database search programs. *Nucleic Acids Res.* 25, 3389–3402.
- Aspenstrom, P., Lindberg, U., and Hall, A. (1996). Two GTPases, Cdc42 and Rac, bind directly to a protein implicated in the immunodeficiency disorder Wiskott-Aldrich syndrome. *Curr. Biol.* 6, 70–75.
- Banin, S., Truong, O., Katz, D.R., Waterfield, M.D., Brickell, P.M., and Gout, I. (1996). Wiskott-Aldrich syndrome protein (WASp) is a binding partner for c-Src family protein-tyrosine kinases. *Curr. Biol.* 6, 981–988.
- Brakeman, P.R., Lanahan, A.A., O'Brien, R., Roche, K., Barnes, C.A., Haganir, R.L., and Worley, P.F. (1997). Homer: a protein that selectively binds metabotropic glutamate receptors. *Nature* 386, 284–288.
- Brindle, N.P.J., Holt, M.R., Davies, J.E., Price, C.J., and Critchley, D.R. (1996). The focal-adhesion vasodilator-stimulated phosphoprotein (VASP) binds to the proline-rich domain in vinculin. *Biochem. J.* 318, 753–757.
- Brünger, A.T. (1992a). The free R value: a novel statistical quantity for assessing the accuracy of crystal structures. *Nature* 355, 472–474.
- Brünger, A.T. (1992b). X-PLOR, Version 3.1: A System for X-Ray Crystallography and NMR (New Haven, CT: Yale University Press).
- Brünger, A.T., Adams, P.D., Clore, G.M., DeLano, W.L., Gros, P., Grosse-Kunstleve, R.W., Jiang, J.-S., Kuszewski, J., Nilges, M., Pannu, N.S., et al. (1998). Crystallography and NMR system: a new software suite for macromolecular structure determination. *Acta Crystallogr. D* 54, 905–921.
- Bunnell, S.C., Henry, P.A., Kolluri, R., Kirchhausen, T., Rickles, R.J., and Berg, L.J. (1996). Identification of Itk/Tsk Src homology 3 domain ligands. *J. Biol. Chem.* 271, 25646–25656.
- Chakraborty, T., Ebel, F., Domann, E., Niebuhr, K., Gerstel, B., Pistor, S., Temm-Grove, C.J., Jockusch, B.M., Reinhard, M., Walter, U., and Wehland, J. (1995). A focal adhesion factor directly linking intracellularly motile *Listeria monocytogenes* and *Listeria ivanovii* to the actin-based cytoskeleton of mammalian cells. *EMBO J.* 14, 1314–1321.
- Collaborative Computational Project Number 4 (1994). The CCP4 suite: programs for protein crystallography. *Acta Crystallogr. D* 50, 760–763.

- Cory, G.O., MacCarthy-Morrogh, L., Banin, S., Gout, I., Brickell, P.M., Levinsky, R.J., Kinnon, C., and Lovering, R.C. (1996). Evidence that the Wiskott-Aldrich syndrome protein may be involved in lymphoid cell signaling pathways. *J. Immunol.* *157*, 3791–3795.
- Derry, J.M.J., Ochs, H.D., and Francke, U. (1994). Isolation of a novel gene mutated in Wiskott-Aldrich syndrome. *Cell* *78*, 635–644.
- Fedorov, A.A., Fedorov, E., Gertler, F., and Almo, S.C. (1999). Structure of EVH1, a novel proline-rich ligand-binding module involved in cytoskeletal dynamics and neural function. *Nat. Struct. Biol.* *6*, 661–666.
- Feng, S., Chen, J.K., Yu, H., Simon, J.A., and Schreiber, S.L. (1994). Two binding orientations for peptides to the Src SH3 domain: development of a general model of SH3-ligand interactions. *Science* *266*, 1241–1247.
- Ferguson, K.M., Lemmon, M.A., Schlessinger, J., and Sigler, P.B. (1994). Crystal structure at 2.2 Å resolution of the pleckstrin homology domain from human dynamin. *Cell* *79*, 199–209.
- Gertler, F.B., Niebuhr, K., Reinhard, M., Wehland, J., and Soriano, P. (1996). Mena, a relative of VASP and Drosophila Enabled, is implicated in the control of microfilament dynamics. *Cell* *87*, 227–239.
- Goelet, P., Castellucci, V.F., Schacher, S., and Kandel, E.R. (1986). The long and the short of long-term memory—a molecular framework. *Nature* *322*, 419–422.
- Hall, T.M.T., Porter, J.A., Young, K.E., Koonin, E.V., Beachy, P.A., and Leahy, D.J. (1997). Crystal structure of a Hedgehog autoprocessing domain: homology between Hedgehog and self-splicing proteins. *Cell* *91*, 85–97.
- Jones, T.A., Zou, J.Y., Cowan, S.W., and Kjeldgaard, M. (1991). Improved methods for the building of protein models in electron density maps and the location of errors in these models. *Acta Crystallogr.* *A47*, 110–119.
- Kato, A., Ozawa, F., Saitoh, Y., Hirai, K., and Inokuchi, K. (1997). *ves1*, a gene encoding VASP/Ena family related protein, is upregulated during seizure, long-term potentiation and synaptogenesis. *FEBS Lett.* *412*, 183–189.
- Kato, A., Ozawa, F., Saitoh, Y., Fukazawa, Y., Sugiyama, H., and Inokuchi, K. (1998). Novel members of the Ves/Homer family of PDZ proteins that bind metabotropic glutamate receptors. *J. Biol. Chem.* *273*, 23969–23975.
- Kirchhausen, T. (1998). Wiskott-Aldrich syndrome: a gene, a multi-functional protein and the beginnings of an explanation. *Mol. Med. Today* *4*, 300–304.
- Kolluri, R., Toliás Fuchs, K., Carpenter, C.L., Rosen, F.S., and Kirchhausen, T. (1996). Direct interaction of the Wiskott-Aldrich syndrome protein with the GTPase Cdc42. *Proc. Natl. Acad. Sci. USA* *93*, 5615–5618.
- Kraulis, P.J. (1991). MOLSCRIPT: a program to produce both detailed and schematic plots of protein structures. *J. Appl. Cryst.* *24*, 946–950.
- Kuriyan, J., and Cowburn, D. (1997). Modular peptide recognition domains in eukaryotic signaling. *Annu. Rev. Biophys. Biomol. Struct.* *26*, 259–288.
- Kurtz, J., Berger, A., and Katchalski, E. (1956). Mutarotation of poly-L-proline. *Nature* *178*, 1066–1067.
- Lanier, L.M., Gates, M.A., Witke, W., Menzies, S.A., Wehman, A.M., Macklis, J.D., Kwiatkowski, D., Soriano, P., and Gertler, F. (1999). Mena is required for neurulation and commissure formation. *Neuron* *22*, 313–325.
- Laskowski, R.A., MacArthur, M.W., Moss, D.S., and Thornton, J.M. (1993). PROCHECK: a program to check the stereochemical quality of protein structures. *J. Appl. Cryst.* *26*, 283–291.
- Laurent, V., Loisel, T.P., Harbeck, B., Wehman, A., Grobe, L., Jockusch, B.M., Wehland, J., Gertler, F.B., and Carlier, M.-F. (1999). Role of proteins of the Ena/VASP family in actin-based motility of *Listeria monocytogenes*. *J. Cell. Biol.* *144*, 1245–1258.
- Lemmon, M.A., and Ferguson, K.M. (1998). Pleckstrin homology domains. *Curr. Topics Microbiol. Immunol.* *228*, 39–74.
- Macias, M.J., Musacchio, A., Ponstingl, H., Nilges, M., Saraste, M., and Oschkinat, H. (1994). Structure of the pleckstrin homology domain from beta-spectrin. *Nature* *369*, 675–677.
- Macias, M.J., Hyvönen, M., Baraldi, E., Schultz, J., Sudol, M., Saraste, M., and Oschkinat, H. (1996). Structure of the WW domain of a kinase-associated protein complexed with a proline-rich peptide. *Nature* *382*, 646–649.
- Mahoney, N.M., Rozwarski, D.A., Fedorov, E., Fedorov, A.A., and Almo, S.C. (1999). Profilin binds proline-rich ligands in two distinct amide backbone orientations. *Nat. Struct. Biol.* *6*, 666–671.
- Miki, H., and Takenawa, T. (1998). Direct binding of the verprolin-homology domain in N-WASP to actin is essential for cytoskeletal reorganization. *Biochem. Biophys. Res. Comm.* *243*, 73–78.
- Miki, H., Miura, K., and Takenawa, T. (1996). N-WASP, a novel actin-depolymerizing protein, regulates the cortical cytoskeletal rearrangement in a PIP2-dependent manner downstream of tyrosine kinases. *EMBO J.* *15*, 5326–5335.
- Musacchio, A., Saraste, M., and Wilmanns, M. (1994). High-resolution crystal structures of tyrosine kinase SH3 domains complexed with proline-rich peptides. *Nat. Struct. Biol.* *1*, 546–551.
- Naisbitt, S., Kim, E., Tu, J.C., Xiao, B., Sala, C., Valtschanoff, J., Weinberg, R., Worley, P., and Sheng, M. (1999). Shank, a novel family of postsynaptic density proteins that binds to the NMDA receptor/PSD-95/GKAP complex and cortactin. *Neuron* *23*, 569–582.
- Navaza, J. (1994). AMoRe: an automated package for molecular replacement. *Acta Crystallogr.* *A50*, 157–163.
- Nicholls, A., Sharp, K.A., and Honig, B. (1991). Protein folding and association: insights from the interfacial and thermodynamic properties of hydrocarbons. *Proteins: Struct. Func. Genet.* *11*, 281–296.
- Niebuhr, K., Ebel, F., Frank, R., Reinhard, M., Domann, E., Carl, U.D., Walter, U., Gertler, F.B., Wehland, J., and Chakraborty, T. (1997). A novel proline-rich motif present in ActA of *Listeria monocytogenes* and cytoskeletal proteins is the ligand for the EVH1 domain, a protein module present in the Ena/VASP family. *EMBO J.* *16*, 5433–5444.
- Nonoyama, S., and Ochs, H.D. (1998). Characterization of the Wiskott-Aldrich syndrome protein and its role in the disease. *Curr. Opin. Immunol.* *10*, 407–412.
- Otwinowski, Z., and Minor, W. (1997). Processing of X-ray diffraction data collected in oscillation mode. *Meth. Enzymol.* *276*, 307–326.
- Pannu, N.S., and Read, R.J. (1996). Improved structure refinement through maximum likelihood. *Acta Crystallogr.* *A52*, 659–668.
- Petrella, E.C., Machesky, L.N., Kaiser, D.A., and Pollard, T.D. (1996). Structural requirements and thermodynamics of the interaction of proline peptides with profilin. *Biochemistry* *35*, 16535–16543.
- Ponting, C.P., and Phillips, C. (1997). Identification of homer as a homologue of the Wiskott-Aldrich syndrome protein suggests a receptor-binding function for WH1 domains. *J. Molec. Med.* *75*, 769–771.
- Prehoda, K.E., Lee, D.J., and Lim, W.A. (1999). Structure of the enabled/VASP homology 1 domain-peptide complex: a key component in the spatial control of actin assembly. *Cell* *97*, 471–480.
- Purich, D.L., and Southwick, F.S. (1997). ABM-1 and ABM-2 homology sequences: consensus docking sites for actin-based motility defined by oligoproline regions in *Listeria ActA* surface protein and human VASP. *Biochem. Biophys. Res. Comm.* *231*, 686–691.
- Ramesh, N., Anton, I.M., Hartwig, J.H., and Geha, R.S. (1997). WIP, a protein associated with Wiskott-Aldrich syndrome protein, induces actin polymerization and redistribution in lymphoid cells. *Proc. Natl. Acad. Sci. USA* *94*, 14671–14676.
- Ramesh, N., Anton, I.M., Martinez-Quiles, N., and Geha, R.S. (1999). Waltzing with WASP. *Trends Cell Biol.* *9*, 15–19.
- Read, R.J. (1986). Improved Fourier coefficients for maps using phases from partial structures with errors. *Acta Crystallogr.* *A42*, 140–149.
- Reinhard, M., Halbrugge, M., Scheer, U., Wiegand, C., Jockusch, B.M., and Walter, U. (1992). The 46/50 kDa phosphoprotein VASP purified from human platelets is a novel protein associated with actin filaments and focal contacts. *EMBO J.* *11*, 2063–2070.
- Reinhard, M., Jouvenal, K., Tripiet, D., and Walter, U. (1995). Identification, purification, and characterization of a zyxin-related protein that binds the focal adhesion and microfilament protein VASP (vasodilator-stimulated phosphoprotein). *Proc. Natl. Acad. Sci. USA* *92*, 7956–7960.

- Rivero-Lezcano, O.M., Marcilla, A., Sameshima, J.H., and Robbins, K.C. (1995). Wiskott-Aldrich syndrome protein physically associates with Nck through Src homology 3 domains. *Mol. Cell Biol.* **15**, 5725–5731.
- Schwartz, K. (1996). WASPbase: a database of WAS- and XLT-causing mutations. *Immunol. Today* **17**, 496–502.
- She, H.Y., Rockow, S., Tang, J., Nishimura, R., Skolnik, E.Y., Chen, M., Margolis, B., and Li, W. (1997). Wiskott-Aldrich syndrome protein is associated with the adapter protein Grb2 and the epidermal growth factor receptor in living cells. *Mol. Biol. Cell* **8**, 1709–1721.
- Smith, G.A., Theriot, J.A., and Portnoy, D.A. (1996). The tandem repeat domain in the *Listeria monocytogenes* ActA protein controls the rate of actin-based motility, the percentage of moving bacteria, and the localization of vasodilator-stimulated phosphoprotein and profilin. *J. Cell Biol.* **135**, 647–660.
- Sone, M., Hoshino, M., Suzuki, E., Kuroda, S., Kaibuchi, K., Nakagoshi, H., Saigo, K., Nabeshima, Y., and Hama, C. (1997). Still life, a protein in synaptic terminals of *Drosophila* homologous to GDP-GTP exchangers. *Science* **275**, 543–547.
- Stapley, B.J., and Creamer, T.P. (1999). A survey of left-handed polyproline II helices. *Protein Sci.* **8**, 587–595.
- Stewart, D.M., Tian, L., and Nelson, D.L. (1999). Mutations that cause the Wiskott-Aldrich Syndrome impair the interaction of Wiskott-Aldrich Syndrome protein (WASP) with WASP Interacting Protein. *J. Immunol.* **162**, 5019–5024.
- Sun, J., Tadokoro, S., Imanaka, T., Murakami, S.D., Nakamura, M., Kashiwada, K., Ko, J., Nishida, W., and Sobue, K. (1998). Isolation of PSD-Zip45, a novel Homer/ves1 family protein containing leucine zipper motifs, from rat brain. *FEBS Lett.* **437**, 304–308.
- Symons, M., Derry, J.M., Karlak, B., Jiang, S., Lemahieu, V., McCormick, F., Francke, U., and Abo, A. (1996). Wiskott-Aldrich syndrome protein, a novel effector for the GTPase CDC42Hs, is implicated in actin polymerization. *Cell* **84**, 723–734.
- Tadokoro, S., Tachibana, T., Imanaka, T., Nishida, W., and Sobue, K. (1999). Involvement of unique leucine-zipper motif of PSD-Zip45 (Homer 1c/ves1-1L) in group 1 metabotropic glutamate receptor clustering. *Proc. Natl. Acad. Sci. USA* **96**, 13801–13806.
- Terwilliger, T.C., and Eisenberg, D. (1983). Unbiased three-dimensional refinement of heavy-atom parameters by correlation of origin-removed Patterson functions. *Acta Crystallogr.* **A39**, 813–817.
- Terwilliger, T.C., and Berendzen, J. (1997). Bayesian MAD phasing. *Acta Crystallogr.* **D53**, 571–579.
- Tu, J.C., Xiao, B., Yuan, J.P., Lanahan, A.A., Loeffert, K., Li, M., Linden, D.J., and Worley, P.F. (1998). Homer binds a novel proline-rich motif and links group 1 metabotropic glutamate receptors with IP3 receptors. *Neuron* **21**, 717–726.
- Tu, J.C., Xiao, B., Naisbitt, S., Yuan, J.P., Petralia, R.S., Brakeman, P., Doan, A., Aakalu, V.K., Lanahan, A., Sheng, M., and Worley, P.F. (1999). Coupling of mGluR/Homer and PSD-95 complexes by the Shank family of postsynaptic density proteins. *Neuron* **23**, 583–592.
- Wills, Z., Bateman, J., Korey, C.A., Comer, A., and Van Vactor, D. (1999). The tyrosine kinase Abl and its substrate Enabled collaborate with the receptor phosphatase Dlar to control motor axon guidance. *Neuron* **22**, 301–312.
- Wlodawer, A., Hodgson, K.O., and Shooter, E.M. (1975). Crystallization of nerve growth factor from mouse submaxillary glands. *Proc. Natl. Acad. Sci. USA* **72**, 777–779.
- Xiao, B., Tu, J.C., Petralia, R.S., Yuan, J.P., Doan, A., Breder, C.D., Ruggiero, A., Lanahan, A.A., Wenthold, R.J., and Worley, P.F. (1998). Homer regulates the association of group 1 metabotropic glutamate receptors with multivalent complexes of Homer-related, synaptic proteins. *Neuron* **21**, 707–716.
- Yoon, H.S., Hajduk, P.J., Petros, A.M., Olejniczak, E.T., Meadows, R.P., and Fesik, S.W. (1994). Solution structure of a pleckstrin homology domain. *Nature* **369**, 672–675.
- Yu, H., Chen, J.K., Feng, S., Dalgarno, D.C., Brauer, A.W., and Schreiber, S.L. (1994). Structural basis for the binding of proline-rich peptides to SH3 domains. *Cell* **76**, 933–945.
- Zhang, Z., Schaffer, A.A., Miller, W., Madden, T.L., Lipman, D.J., Koonin, E.V., and Altschul, S.F. (1998). Protein sequence similarity searches using patterns as seeds. *Nucleic Acids Res.* **26**, 3986–3990.
- Zhou, M.M., Ravichandran, K.S., Olejniczak, E.F., Petros, A.M., Meadows, R.P., Sattler, M., Harlan, J.E., Wade, W.S., Burakoff, S.J., and Fesik, S.W. (1995). Structure and ligand recognition of the phosphotyrosine binding site of Shc. *Nature* **378**, 584–592.
- Zhu, Q., Watanabe, C., Liu, T., Hollenbaugh, D., Blaese, R.M., Kanter, S.B., Aruffo, A., and Ochs, H.D. (1997). Wiskott-Aldrich syndrome/X-linked thrombocytopenia: WASP gene mutations, protein expression, and phenotype. *Blood* **90**, 2680–2689.

Protein Data Bank Accession Numbers

Atomic coordinates and structure factor amplitudes for the liganded and unliganded structures have been deposited in the Protein Data Bank for release upon publication (accession codes 1DDV and 1DDW, respectively).